

Electronic properties of two- and three-dimensional quasicrystalline model systems in a magnetic field

H. Schwabe, G. Kasner, and H. Böttger

Institut für Theoretische Physik, Otto-von-Guericke-Universität Magdeburg, Postschließfach 4120, 39016 Magdeburg, Germany

(Received 5 November 1996; revised manuscript received 4 June 1997)

The density of states as a function of the magnetic field and the magnetoconductance of two- and three-dimensional quasicrystalline model systems are calculated in a simple tight-binding description. The zero-field spectra are known to show a very complicated spiky structure with many small gaps. A magnetic field leads to a more uniform distribution of the states. Correspondingly, the energy regions showing finite values for the magnetoconductance as a function of the Fermi energy become larger with a growing field. The investigation of the high-field behavior uncovers an interesting structure of the spectra quasiperiodic with the field. This quasiperiod can be explained as a simple interference of periods in the incommensurable ratio of the areas perpendicular to the flux contained in the cluster. [S0163-1829(97)00237-3]

I. INTRODUCTION

Since the discovery of quasicrystals many authors found experimentally very exotic behavior of some of their physical properties.^{1,2} They show, for instance, a very low electrical conductance depending strongly on the composition.³ In theoretical studies simple model systems were used to find the origin of these properties in the quasicrystalline structure.⁴⁻¹³ A well investigated one-dimensional model—the Fibonacci chain—has a singular continuous spectrum and the corresponding wave functions are neither exponentially localized nor extended but critical.⁴ An example of a two-dimensional quasicrystal is the Penrose lattice. Most of the wave functions are believed to be critical too, but some highly degenerated strongly localized states, so-called confined states, have been found.^{4-9,15} In a tight-binding picture the conductance as a function of the Fermi energy shows very strong fluctuations and even energy ranges having zero conductance.¹⁰ This can be explained by a very irregular distribution of the states contributing to the conductance. First calculations for a three-dimensional icosahedral model system exhibit qualitatively the same behavior.⁶ Some work has been done introducing a magnetic field to quasicrystalline model systems.^{15,16} Very interesting properties have been found, for instance, a quasiperiodic structure in the magnetic-field dependence of the spectrum for the Penrose lattice.¹⁶

We present some more systematic theoretical investigations of electronic properties of two- and three-dimensional quasicrystals in a magnetic field comparing the results of a few simple but significant example models. First we introduce the model systems. The next sections give an overview of our results for the magnetoconductance based on the density of states. A further section deals with the detailed investigation of the spectra as a function of the magnetic field. The quasiperiodic repetition of significant structure elements in the spectra with increasing field can be explained as a simple interference of periods in the ratio of the areas perpendicular to the flux contained in the cluster. To show this, we perform a Fourier analysis for the plots of some selected

eigenvalues as a function of the magnetic field. We find only very few frequencies in the positions of the areas in the cluster. Finally we draw some conclusions.

II. MODEL

We used a very simple standard model describing only the quasicrystalline structure but no other physical effects of real materials (see, for instance, Ref. 4). The main features are to use mesoscopic clusters at zero temperature being small enough to avoid inelastic scattering, lattices in a tight-binding approximation with s -like atom functions localized at the lattice sites and open boundary conditions. To calculate the conductance we have to add an external electric field in the linear-response approximation.¹⁰ Charged particles are spinless and noninteracting electrons. Two leads of undisturbed material being infinitely long but of finite width and outside of the magnetic field serve as electronic reservoirs. The calculation is done via the Landauer formula $\Gamma = (e^2/h)\hat{t}\hat{t}^\dagger$, where \hat{t} is the transmission matrix of states of the undisturbed lead, scattered elastically at the quasicrystalline cluster.

A. Hamiltonian in a magnetic field

The Hamiltonian H describing a quasicrystalline cluster reads in the tight-binding representation

$$H = \sum_{ij} V_{ij}|i\rangle\langle j| \quad i, j \text{ NN} \quad (1)$$

with the transfer integrals between the next-neighbor sites i and j without a magnetic field

$$V_{ij} = \int d\vec{r} \phi_i^*(\vec{r} - \vec{R}_i) H \phi_j(\vec{r} - \vec{R}_j) \equiv V_{ij}(0) = 1, \quad (2)$$

$\phi_j(\vec{r} - \vec{R}_j)$ denotes the s -like atom function at lattice site j .

The introduction of a magnetic field is done by $H(\vec{p}) \rightarrow H(\vec{p} - e\vec{A})$ with the vector potential \vec{A} belonging to the magnetic field $\vec{B} = B\vec{e}_z$. The atom function at site j in the magnetic field is¹⁴

$$\phi_i(\vec{r}, \vec{R}_i, B) = \chi_i(\vec{r} - \vec{R}_i, B) e^{(ie/\hbar)\vec{A}(\vec{r})\vec{R}_i},$$

$$\chi_i(\vec{r} - \vec{R}_i, B) \approx \chi_i(\vec{r} - \vec{R}_i) \quad (3)$$

with the elementary charge e and Planck's constant \hbar . The approximation neglects the shrinking of the wave function in very strong magnetic fields. The integrals of the transfer energy (2) in the field get the form

$$V_{ij}(B) = \int d\vec{r} e^{(ie/\hbar)\vec{A}(\vec{r})(\vec{R}_j - \vec{R}_i)} \chi_i^*(\vec{r} - \vec{R}_i) H \chi_j(\vec{r} - \vec{R}_j)$$

$$\approx e^{i(e/2\hbar)\vec{A}(\vec{R}_i + \vec{R}_j)(\vec{R}_j - \vec{R}_i)}. \quad (4)$$

This approximation is valid for overlap functions $\chi_i^*(\vec{r} - \vec{R}_i) H \chi_j(\vec{r} - \vec{R}_j)$ localized midway between site i and j .

In the following we use the Landau gauge $\vec{A}(\vec{r}) = -yB\vec{e}_x$. Then the transfer energy (4) becomes

$$V_{ij}(B) = e^{ib(x_i - x_j)(y_i + y_j)}, \quad b \equiv \frac{eB}{2\hbar} \rightarrow ba_0^2 = \frac{\Phi}{2\Phi_0}. \quad (5)$$

Here $\Phi_0 = h/2e$ is the flux quantum and $\Phi = \pi a_0^2 B$ is the flux at the field B through an area πa_0^2 with $a_0 \equiv 1$ the lattice constant. So b denotes the value of the magnetic flux through the elementary cells of the lattice in units of Φ_0 , that is, b measures the strength of the magnetic field in a dimensionless form.

B. Two- and three-dimensional quasicrystalline clusters

The most investigated two-dimensional quasiperiodic structure is the Penrose lattice. Its prototiles are two sorts of rhombuses. We use it in two ways. The first one is to set an atom at every vertex point to get the so-called vertex model (PVM). The second model is the center model (PCM) with one atom lying in the center of each rhombus. Both models have several interesting opposite features, well summarized in Ref. 4. The coordination number of the PVM varies from 3 to 7 for the several vertex stars and the model is bipartite. As a consequence the density of states has to be symmetric around $E=0$ in a band of $-7 < E < 7$. The PCM has a uniform coordination number of 4 at every site and is not bipartite leading to an asymmetric density of states (DOS).

A three-dimensional model with similar features is the model described by Danzer¹⁷ which may serve as a model for real icosahedral quasicrystals of high quality such as Al-Pd-Mn or Al-Cu-Fe. It has several tetrahedra as prototiles. Again we can define a vertex model (IVM) with atoms at the edges of the tetrahedra and a center model (ICM) with an atom situated in the middle of each tetrahedron.⁶ Also for the icosahedral system the center model has a uniform coordination number of 4, while this for the IVM varies up to 62. But in opposition to the Penrose lattice, the ICM is bipartite but not the IVM.

We calculated some electronic properties for one example of each of these 4 models. Specifically we used a piece of a Penrose-8/5-approximate having 473 sites for the PVM and 378 sites for the PCM for the two-dimensional calculations and a triacontahedron-shaped cluster of the Danzer model in the third deflation level having 1069 sites for the IVM and

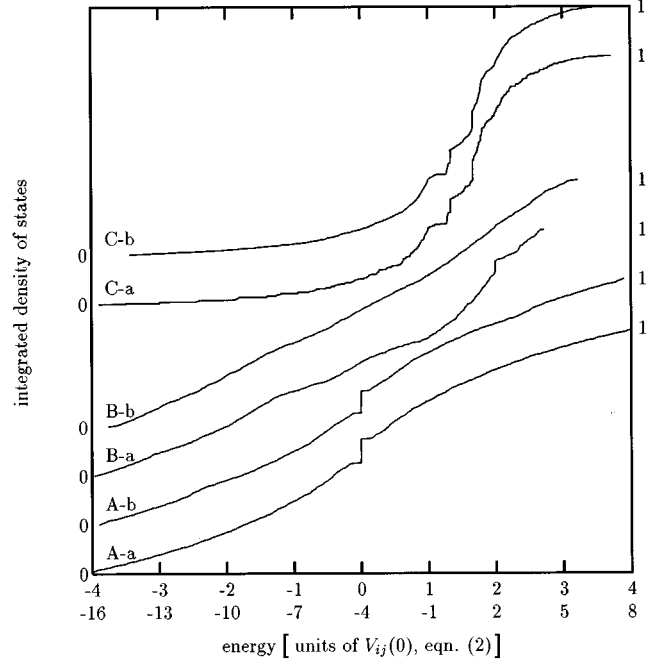


FIG. 1. Integrated density of states of (A) PVM, (B) PCM, (C) IVM: (a) without a magnetic field $b=0$ and (b) in a field $b=0.5$, the lower axis of energy is valid for (A) and (B), the upper one is valid for (C).

4320 sites for the ICM for the three-dimensional one. In the following sections we show the results and compare it for several models.

III. DENSITY OF STATES AND MAGNETOCONDUCTANCE

The density of states (DOS) in quasicrystalline systems is known to show a very irregular structure with energy regions containing clusters of discrete states and other regions having no or just a few isolated states. This behavior is proven even analytically for the one-dimensional quasicrystalline Fibonacci chain, where the DOS forms a cantor-set-like fractal structure.⁴ The DOS for two-^{4,5} and three-dimensional⁶ quasicrystalline models seems to be more complicated but of fractal structure. Calculating the conductance of the same systems as a function of the Fermi energy as a parameter one finds that the complicated structure of the DOS is recovered. That is, the system shows conductivity only in a small surrounding region of any state. If there is another state in this region, a conducting band arises. Certainly, the width of this region depends on the size of the finite cluster. It becomes smaller with increasing size. But computational results suggest that the additional states of a larger system are also arranged in many small clusters rather than showing a uniform distribution over the whole energy range, leading to very spiky DOS and conductance plots. Formation of wide energy bands as in periodic systems cannot be observed.

Now we introduce a magnetic field to our quasicrystalline models and calculate the DOS and the conductance again. We find, that an increasing strength of the magnetic field leads to a more uniform distribution of states. In Fig. 1 the integrated DOS in a magnetic field of strength $b=0.5$ (graph b) is compared to that without a field (graph a) for some of

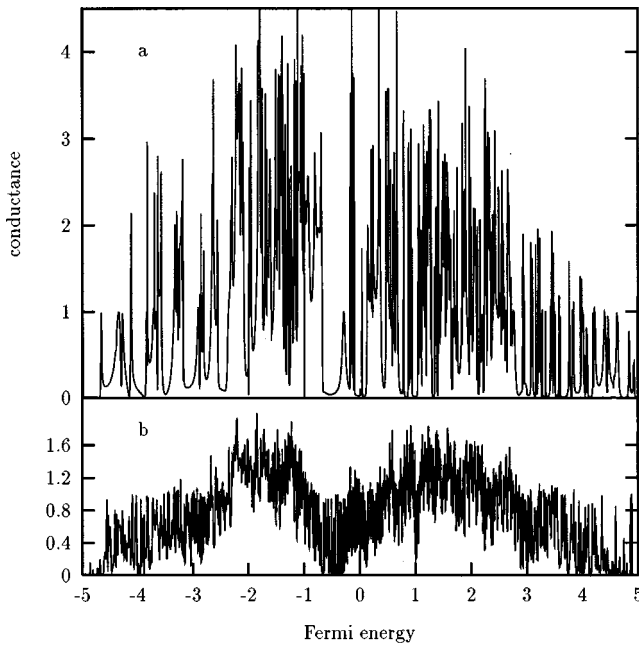


FIG. 2. Conductance as a function of the Fermi energy for the IVM: (a) without a magnetic field $b=0$ and (b) in a field of strength $b=0.5$.

our model systems. Generally, the curves in the field are much smoother, more linear, and get smaller steps. Additionally, for the PVM (graphs A) it is seen that the high degeneracy of the confined states at $E=0$ also occur in the field. This is not the case for the PCM (graphs B) at $E=2$ and, not to be seen so clearly, for the IVM (graphs C) at $E=0$. We will return to this point later.

Corresponding to the uniform distribution of states we also find much smoother conductance plots. That is, the absolute value of the highest peaks in the plot become lower but there arise larger conducting energy regions. As an example, for the development of the conductance in a magnetic field, we show the plot for the IVM in Fig. 2, without a magnetic field in graph (a) and in a field of strength $b=0.5$ in graph (b).

The behavior of the DOS and the conductance in a magnetic field can be regarded as being very similar to the behavior of eigenstates in fractal lattices.¹⁸ There a magnetic field leads to a spread of highly degenerated localized states to new extended states because of the broken structural symmetry due to the field. In the case of our models, we have not degenerated but some clusters of very closely distributed states at several energy regions without a field. An exception are some highly degenerated so-called confined states being strongly localized at distinct local environments in the quasi-lattice. We found them in three of our four models on integer energy values, but not in the ICM. The total number of states is fixed, so a “spreading” means a more uniform distribution here, rather than new states. Whether the states are localized or extended cannot be determined because of the small size of the cluster. That is, there is no well-defined localization length. An interesting fact is that we observed a true spreading mechanism for the confined states as expected, but not in the bipartite PVM. In this model the confined states turned out to be absolutely stable against even very high magnetic fields, in the sense that their amplitudes

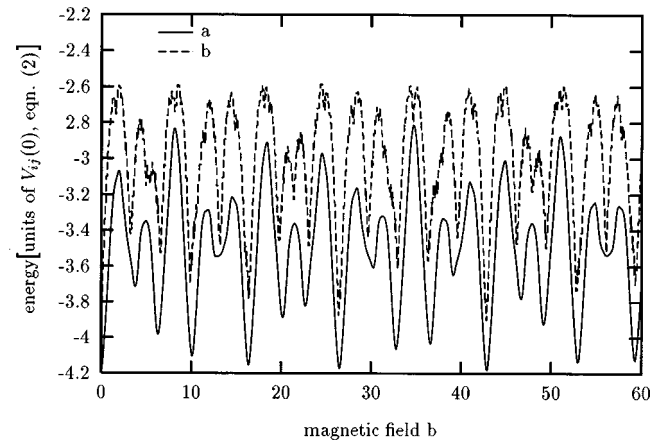


FIG. 3. (a) Lowest eigenvalue of the finite PVM as a function of the magnetic field. (b) $f_{\text{PVM}}(b)=[A \cos(2Ab)+B \cos(2Bb)]/(A+B)$.

remain zero at the sites not yet occupied without a field. It follows that a field does not cause a breaking of any structural symmetry in this case. Generally, confined states in bipartite models are reported as stable,^{4,6–8,16} while that in the nonbipartite models vanish quickly with any disturbance of the structure or in a field.^{8,15}

IV. SPECTRA IN A MAGNETIC FIELD

A very interesting development of the spectrum of the PVM for a growing magnetic field is reported in Ref. 16. Let us define that “plot a spectrum” means to make a point at an energy value if there is a state. Then a plot of the calculated spectrum against the magnetic field strength b uncovers a complicated structure similar to the fractal butterfly-shaped graph introduced by Hofstadter¹⁹ for the square lattice, but showing a quasiperiodically repetition of structure elements, forming a Fibonacci chain for the PVM. A similar behavior was found for the superconducting transition temperature as a function of the applied magnetic field in artificial quasiperiodically arranged systems.²⁰ The interpretation of the clear structure in Ref. 16 was the assumption of Landau band formation in the PVM, as known for the square lattice. We found a somewhat different behavior investigating the other models. To be sure, we discovered a quasiperiodic structure for the width of the band for the ICM, too. But for our nonbipartite models it is the position of the band rather than its width that changes quasiperiodically. Additionally, a clear structure within the band could be seen only for the PVM. Here, we denote a band as a region between the lowest and the highest eigenvalue.

To analyze this behavior we limit our investigations to the eigenvalues at the band edge. Let us start with the PVM. Because this model is bipartite, we only have to look at the lowest eigenvalue $\epsilon(b)$. It is plotted as a function of the magnetic field in curve (a) of Fig. 3. One can see the typical quasiperiodic Fibonacci chain structure in the repetition of peaks and dips as reported in Ref. 8. Because the highest eigenvalue is mirror symmetric to the lowest one, this means that the width of the band changes quasiperiodically with the magnetic field. As it is shown by the plot of the simple function $f_{\text{PVM}}(b)=[A \cos(2Ab)+B \cos(2Bb)]/(A+B)$ in

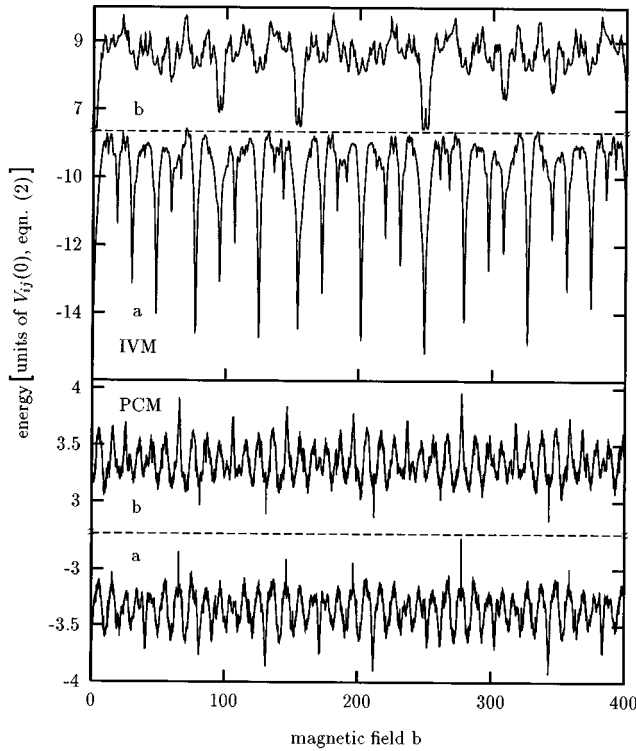


FIG. 4. (a) Lowest and (b) highest eigenvalue of the nonbipartite models PCM and IVM as a function of the magnetic field b .

curve (b) in Fig. 3, this structure can be declared by the incommensurable ratios of the areas A and B of closed loops perpendicular to the flux in the PVM. Here $A = \sin(2/5\pi)$ and $B = \sin(1/5\pi)$ are the areas of thick and thin rhombuses in the PVM having the golden ratio $A/B = \tau = [\sqrt{5} + 1]/2$. Also the ratio of the number of rhombuses is $A/B = \tau$. This simple interference function of the cosine of both areas in the weighted ratio of their occurrence in the model is astonishingly similar to the curve of $\epsilon(b)$.

A more complicated structure was found for the plot of the lowest eigenvalue as a function of the magnetic field for the PCM. Additionally, we found a very similar appearance of the plot for the lowest and the highest eigenvalue in this nonbipartite model, that is, peaks of the highest eigenvalue correspond to dips of the lowest one and vice versa. It follows for the band a shift value changing quasiperiodically with the magnetic field, while the width of the band is nearly fixed. It is plotted in the lower part of Fig. 4.

A similar behavior could be found for the IVM, which is also nonbipartite. But only the main peaks in the lowest eigenvalue have corresponding dips in the highest one and the amplitude is smaller, to be seen in the upper part of Fig. 4. That is, the picture of a fixed bandwidth is only valid as a rough approximation. We have to leave the explanation for the special behavior of nonbipartite models to later investigations.

Suggested by the very similarity of curves (a) and (b) in Fig. 3 for the PVM, as described above, we extend this approach to other quasicrystalline systems by calculating the Fourier transform of the functions $\epsilon(b)$ being the lowest or highest eigenvalue as a function of the magnetic field b for the several models as

$$\tilde{\epsilon}(K) = \left| \int_0^\infty db \epsilon(b) \exp(iKb) \right|. \quad (6)$$

If $\epsilon(b)$ contains only some discrete frequencies K , we must find δ -like peaks in the plot of $\tilde{\epsilon}(K)$ at these values.

To explain this method we start with a simple finite cluster of a square lattice applying open boundary conditions in a magnetic field with the lattice constant $a = 1$. Solving the arising Harper equation

$$[\epsilon_\gamma + 2 \cos(2yb + k_\gamma)] \chi_\gamma(y) + \chi_\gamma(y+1) + \chi_\gamma(y-1) = 0 \quad (7)$$

and plotting the eigenenergy $\epsilon_\gamma(b)$ of this model in the way described above one gets the well-known butterfly-shaped graph introduced by Hofstadter.¹⁹ Again, we only want to investigate the development of the smallest eigenvalue in the magnetic field. The graph is periodic in the magnetic field b with the period of 2π . This can easily be understood noticing that b enters the Harper equation via the phase of the transfer energy (5) multiplied by A being the size of the areas contained in the cluster. So a period of 2π divided by the area size is expected in the graph. These areas are uniform in the square lattice and of size $A = 1$. The physical meaning of this behavior is the quantization of the flux through an area in a cluster. With open boundaries there is not a condition to choose only distinct magnetic field values b . But nevertheless we find peaks in the graph of the eigenvalues as a function of the magnetic field at values satisfying the condition of integer flux quanta per area. It can easily be understood that also magnetic field values of, e.g., half of that size satisfy such a condition. Then the flux through the area of two squares of the lattice has an integer value. So we find peaks also at $2\pi/2$, $2\pi/3$, $2\pi \cdot 2/3$, and so on.

Only the period of 2π and all its subharmonics $n \cdot 2\pi$ are contained in the Fourier transform $\tilde{\epsilon}(K)$ of the eigenvalue as a function of the magnetic field, that we calculated as an example for a cluster of 20×20 atoms. It is suggested by the amplitude, that rectangular areas are preferred by the ‘‘resonance’’ of the flux at the lattice areas. The largest peak is the one at the smallest possible area, the elementary square of the lattice. The amplitude of areas formed by linear chains of squares is decreasing with increasing length. The peak at $n = 5$ has already nearly no amplitude. But there seems to be additional contributions to the amplitude values by rectangular areas of squares. So there are relatively high peaks at $n = 4 \equiv 2 \times 2$, $n = 6 \equiv 2 \times 3$, $n = 8 \equiv 2 \times 4$, and especially at $n = 12 \equiv 2 \times 6$ or 3×4 because of two possible rectangular areas both having contributing ‘‘resonances.’’

As shown already in the graph $\epsilon(b)$ for the PVM itself, it can be nearly recovered similarly, as described for the square lattice, by interference of only two simple cosine waves of the two frequencies belonging to the areas of fat and thin rhombuses A and B in the ratio of the relative distribution in the lattice. Indeed we find that the corresponding peaks are clearly the largest and in the correct ratio in the Fourier transform $\tilde{\epsilon}(K)$ of the lowest eigenvalue as a function of the magnetic field for the PVM, Fig. 5. But additionally there are smaller peaks lying at sums and also differences of the areas A and/or B as in the square lattice. Note that difference peaks are not distinguished in the square lattice. Again the magni-

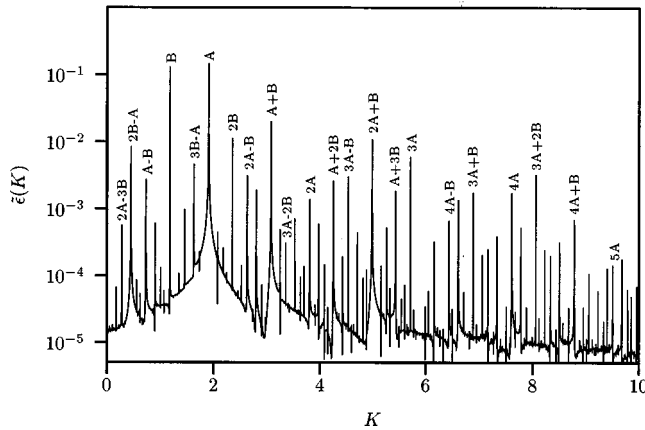


FIG. 5. Fourier transform $\bar{\epsilon}(K)$ of the lowest eigenvalue as a function of the magnetic field in the PVM in logarithmic representation, main peaks are labeled with the areas of resonance.

tude of the subharmonic peaks decreases with the number of included areas in the sum, that is, with higher indices. But some peaks are unexpectedly small, as for instance, 2A compared to the line 3A,4A,5A. We suppose these area combinations are rare in the cluster or have other reasons to be not very important.

Because of the incommensurable proportion of A and B peaks are densely distributed on the K axis. Particularly, peaks with higher indices do not lie necessarily at higher values of K , in contrast to the case of the square lattice. Instead the distribution of high and low peaks shows a fractal-like behavior. Because the PVM is bipartite, the highest eigenvalue as a function of the magnetic field must be the negative of the smallest one and so the absolute value of the Fourier transform has to be identical.

The very dominant magnitude of the main peaks belonging to the basic rhombuses of the Penrose lattice suggests that the subharmonics do not play such an important role in this case. Note that we used a logarithmic scale in Fig. 5. We assume that it saves the formation of Landau bands in the PVM as a nearly undisturbed interference of that of only two periodic systems with lattice constants A and B , respectively. This behavior cannot be found for the other model systems to which we now turn.

We test the behavior of the nonbipartite PCM. First, we have to know the occurring areas and the relative distribution in the Penrose lattice. The lattice consists of seven vertex stars A, B, \dots, G (Ref. 8) and every one of them is related to a distinct polygonal area of the PCM as shown in Fig. 6 by the gray shaded areas.

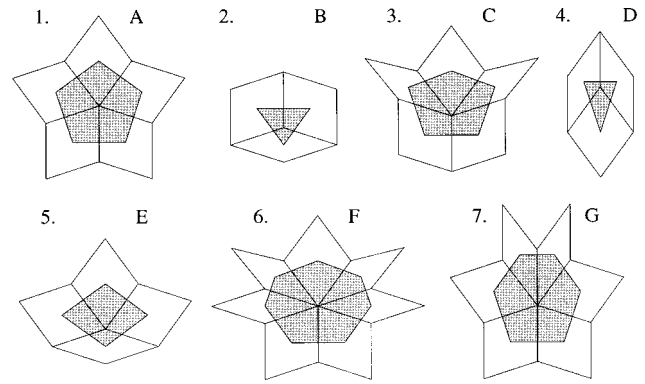


FIG. 6. Allowed vertex stars in the Penrose lattice, the gray shaded areas are the assigned areas in the PCM.

The number of edges is equal to the coordination number of the vertex star. In Table I it is listed together with the relative distribution D_1, D_2, \dots, D_7 in the Penrose lattice and the size A_1, A_2, \dots, A_7 of the related areas, both as an absolute value for a chosen lattice constant of $a = 1$ and relative to the smallest existing area connected with vertex star D .

Note, that the vertex star A here is the summary of the fivefold vertex stars S and $S5$ (Ref. 21) both occurring in the Penrose lattice, arising from different vertex classes but having the same shape and size. Here only geometric properties enter our meditation.

The Fourier spectrum of the function $f_{\text{PCM}}(b) = \sum_{j=1}^7 D_j \cos(A_j b)$ defined analog to $f_{\text{PVM}}(b)$ [note, that $\sum_{j=1}^7 D_j = 1$ (Ref. 8)] is plotted as curve (b) in Fig. 7. The comparison with the Fourier analysis of the smallest eigenvalue of the PCM, plotted with a logarithmic scale in curve (a), shows that the resonances of the two smallest areas A_4 and A_2 are recovered exactly in the correct magnitude and ratio. The third largest area A_5 leads to a peak of around 50% of the amplitude as suggested by its relative distribution in the lattice. The most remarkable behavior is the peak belonging to A_3 . The amplitude does not even reach 5% of its distribution although it is with about 23% the second most frequent vertex star in the lattice. The peaks of the larger vertex stars A, F , and G can be found in the Fourier spectrum with about 20% of the expected amplitude. But all these areas are relatively rare distributed in the lattice. That means the resonance of the large areas in a magnetic field does not play any important role here.

TABLE I. Distribution and the corresponding areas in the center model of the allowed vertex stars in the Penrose lattice Fig. 6.

Number of the vertex star	1	2	3	4	5	6	7
Label of the vertex star	A	B	C	D	E	F	G
Coordination number	5	3	5	3	4	7	6
Distribution in the lattice	τ^{-6}	τ^{-2}	τ^{-3}	τ^{-4}	τ^{-5}	τ^{-6}	τ^{-7}
After Ref. 8	5.57	38.20	23.61	14.59	9.02	5.57	3.44
Corresponding area in the center model	3.112	0.623	2.637	0.532	1.721	4.176	3.644
Relative to the smallest one (vertex 4) in %	585	117	496	100	324	785	685

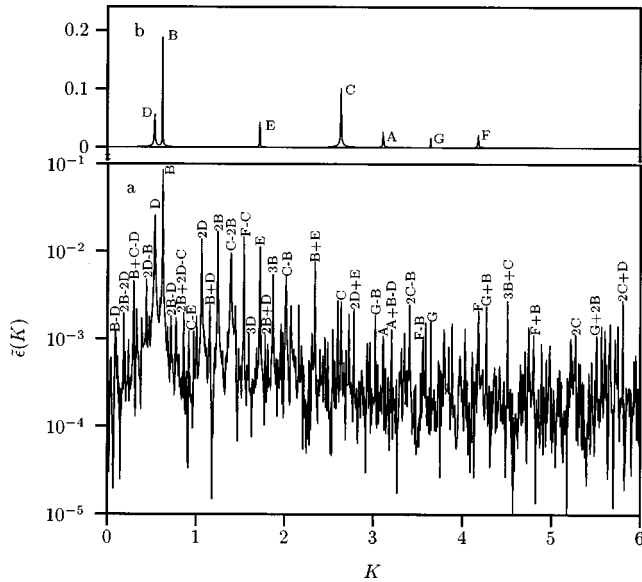


FIG. 7. (a) Fourier transform $\tilde{\epsilon}(K)$ of the lowest eigenvalue as a function of the magnetic field in the PCM in logarithmic representation, main peaks are labeled with the areas of resonance. (b) Fourier transform of $f_{\text{PCM}}(b) = \sum_{j=1}^7 D_j \cos(A_j b)$.

Again subharmonics at sums and differences of the main peaks can be found in the spectrum. Because of the seven basic areas in the cluster there are many more possibilities to get resonant areas compared to the case of the PVM. Indeed some peaks at K values corresponding to sums of even more than two areas are higher than other basic area peaks, e.g., $B + C - D$. This indicates a strong mixing of states. The formation of clear Landau bands should be prevented in this case.

Note that the Fourier analyses of the lowest and the largest eigenvalue for this model are almost identical although the model is not bipartite, in correspondence with the similarity of curve (a) and (b) in the lower part of Fig. 4. Our second nonbipartite system is the IVM. Remember, that we also found very similar functions for the lowest and the highest eigenvalue in dependence on the magnetic field. But in contrast to the PCM, only the main peaks of graph (a) in the upper part of Fig. 4 for the lowest eigenvalue could be found

also in that for the highest one (b). Investigating the Fourier transform of both functions, this behavior is underlined. There are some peaks in $\tilde{\epsilon}(K)$ for the lowest eigenvalue which cannot be found for the highest one. On the other hand, all the peaks of $\tilde{\epsilon}(K)$ for the highest eigenvalue also exist for the lowest one.

The investigation whether the concrete structure of the peaks conforms with areas in the cluster is omitted for the three-dimensional IVM. There is a very large number of various areas in the Danzer model. Moreover because of several angles to the relevant z axis of every area according to the direction of the magnetic-field vector, the number of effective areas perpendicular to the magnetic flux is even larger. Here we only mention that we find again only some discrete frequencies with significant amplitudes suggesting a fixed set of resonant areas in the cluster.

V. CONCLUSIONS

We have investigated magnetic spectra and the magnetoconductance of finite two- and three-dimensional quasicrystalline model systems in a tight-binding description. Generally, there is a trend of the eigenstates to get a more uniform distribution over the whole energy band with increasing magnetic field. Correspondingly, the very small Fermi energy regions of the clusters showing finite conductance without a field become wider in an increasing field. The width of the band in the bipartite models, respectively, the position in the nonbipartite models changes quasiperiodically with the magnetic-field strength. This is due to incommensurate ratios of areas perpendicular to the flux inside the quasicrystalline lattice. We can find a clear structure of the spectra inside the band only for the PVM. That means the formation of Landau bands described in Ref. 16 seems to be due to the fact that the PVM consists only of two types of areas perpendicular to the flux. So it can be regarded as an ideal binary lattice not disturbed enough to destroy the Landau bands of the square lattice. With every additional structural unit they vanish more and more. Because the band limits the region of the Fermi energy where the cluster can show finite conductance, the magnetoconductance near the band edge has to be sensitive to the concrete structure of the quasicrystal.

¹D. P. DiVincenzo and P. J. Steinhardt, *Quasicrystals The State of the Art* (World Scientific, Singapore, 1991).
²K. H. Kuo and T. Ninomiya, *Quasicrystals* (World Scientific, Singapore, 1991).
³P. Lindqvist, P. Lanco, C. Berger, A. G. M. Jansen, and F. Cyrot-Lackmann, *Phys. Rev. B* **51**, 4796 (1995).
⁴H. Tsunetsugu, T. Fujiwara, K. Ueda, and T. Tokihiro, *Phys. Rev. B* **43**, 8879 (1991).
⁵T. Fujiwara, *Quasicrystals* (Ref. 2), p. 294.
⁶G. Kasner, H. Schwabe, and H. Böttger, *Phys. Rev. B* **51**, 10 454 (1995).
⁷T. Rieth and M. Schreiber, *Phys. Rev. B* **51**, 15 827 (1995).
⁸T. Odagaki, *Solid State Commun.* **60**, 693 (1986).
⁹T. C. Choy, *Phys. Rev. B* **35**, 1456 (1987).
¹⁰H. Tsunetsugu and K. Ueda, *Phys. Rev. B* **43**, 8892 (1991).

¹¹K. Ueda and H. Tsunetsugu, *Phys. Rev. Lett.* **58**, 1272 (1987).
¹²S. Yamamoto and T. Fujiwara, *Phys. Rev. B* **51**, 8841 (1995).
¹³Y. Jian, *Z. Phys. B* **88**, 141 (1992).
¹⁴H. Böttger and V. v. Bryksin, *Hopping Conduction in Solids* (Akademie-Verlag, Berlin, 1985).
¹⁵M. Arai, T. Tokihiro, and T. Fujiwara, *J. Phys. Soc. Jpn.* **56**, 1642 (1987).
¹⁶T. Hatakeyama and H. Kamimura, *J. Phys. Soc. Jpn.* **58**, 260 (1989).
¹⁷L. Danzer, *Disc. Math.* **76**, 1 (1989).
¹⁸X. R. Wang, *Phys. Rev. B* **53**, 12 035 (1996).
¹⁹D. R. Hofstadter, *Phys. Rev. B* **14**, 2239 (1976).
²⁰A. Behrooz, M. J. Burns, H. Deckman, D. Levine, B. Whitehead, and P. M. Chaikin, *Phys. Rev. Lett.* **57**, 368 (1986).
²¹N. G. de Bruijn, *Mathematics A* **84**, 39 (1981).